ACI MATERIALS JOURNAL TECHNICAL PAPER

Title No. 120-M70

Corrosion Behavior of Conventional and Corrosion-Resistant Steel Reinforcements in High-Performance and Ultra-High-Performance Concrete

by Ben Wang, Abdeldjelil Belarbi, Mina Dawood, and Bora Gencturk

This paper presents the findings of an experimental study on the corrosion performance of both conventional and corrosion-resistant steel reinforcements in normal-strength concrete (NC), high-performance concrete (HPC), and ultra-high-performance concrete (UHPC) columns in an accelerated corrosion-inducing environment for up to 24 months. Half-cell potential (HCP), linear polarization resistance (LPR), and electrochemical impedance spectroscopy (EIS) methods were used to assess the corrosion activities and corrosion rates. The reinforcement mass losses were directly measured from the specimens and compared to the results from electrochemical corrosion rate measurements. It was concluded that UHPC completely prevents corrosion of reinforcement embedded inside, while HPC offers higher protection than NC in the experimental period. Based on electrochemical measurements, the average corrosion rate of mild steel and high-chromium steel reinforcement in NC in 24 months were, respectively, 6.6 and 2.8 times that of the same reinforcements in HPC. In addition, corrosion-resistant steel reinforcements including epoxy-coated reinforcing bar, high-chromium steel reinforcing bar, and stainless-steel reinforcing bar showed excellent resistance to corrosion compared to conventional mild steel reinforcement. There was no active corrosion observed for epoxy-coated and stainless steel reinforcements during the 24 months of the accelerated aging; the average corrosion rateS of high-chromium steel was 50% of that of mild steel in NC based on the electrochemical corrosion measurements; and the average mass loss of high-chromium steel was 47% and 75% of that of mild steel in NC and HPC, respectively. The results also showed that the LPR method might slightly overestimate the corrosion rate. Finally, pitting corrosion was found to be the dominant type of corrosion in both mild and high-chromium steel reinforcements in NC and HPC columns.

Keywords: corrosion; high-performance concrete (HPC); mass loss; steel reinforcement; ultra-high-performance concrete (UHPC).

INTRODUCTION

The corrosion of reinforcing bars is a major problem for reinforced concrete (RC) structures globally, particularly for structures in marine environments and bridges exposed to deicing chemicals. Studies have revealed that chloride attack is the most common cause of the initiation of reinforcement corrosion (ACI Committee 222 2001). Concrete is alkaline in nature with a pore solution pH of 12 to 13, which creates a passive film and protects the reinforcing bars from corrosion. Once chloride penetrates the concrete cover and reaches a specific concentration (chloride threshold), the passive film on the reinforcement surface is damaged locally. Once the passive film breaks down, reinforcement corrosion initiates in the presence of oxygen and water, followed by the consumption of virgin steel and the production of less-dense corrosion products. The corrosion products—such as ferrous hydride, ferric hydroxide, and ferric oxide—have volumes that are two to 10 times that of virgin steel. The volume expansion creates pressure within the concrete, causing concrete cracking, and eventually leading to concrete spalling around the reinforcing bars.

One way to enhance the durability of RC structures in corrosive environments is through the use of corrosion-resistant reinforcing steels and high-performance concretes (HPCs). These corrosion-resistant steel reinforcements include various types of epoxy-coated (EC), high-chromium (HC), and stainless (SS) steel reinforcements. These corrosion-resistant reinforcements either use physical coatings to limit the access of moisture and oxygen or alter the chemical compositions of steel to improve the corrosion resistance. Several studies examined the performance of these corrosion-resistant reinforcements in conventional normal-strength concrete (NC). Results indicated that EC, HC, and SS steel reinforcement exhibit high corrosion resistance (Cui 2003; Darwin et al. 2013; Hansson et al. 2007; Ji 2005; Rizkalla et al. 2005; Wang et al. 2022).

HPCs show improved durability and mechanical properties compared to NC. In recent years, HPC and ultra-high-performance concrete (UHPC) have been developed and used in infrastructure projects. HPC is defined by ACI Committee 363 (2010) as "…a concrete meeting special combinations of performance and uniformity requirements that cannot always be achieved routinely using conventional constituents and normal mixing, placing, and curing practice…," while UHPC is generally considered to have a compressive strength greater than 150 MPa (Graybeal 2006).

Studies have shown that HPC has better durability and corrosion resistance compared to NC. HPC is achieved through a low water-binder ratio (w/b) and the use of supplementary cementitious materials. The reduced water content and the pozzolanic reactions from the supplementary materials result in a denser matrix with low permeability, which significantly delays chloride penetration and reinforcement

ACI Materials Journal, V. 120, No. 6, November 2023.

MS No. M-2023-083, doi: 10.14359/51739153, received April 5, 2023, and reviewed under Institute publication policies.

corrosion rates. Researchers have conducted several studies to investigate the durability and corrosion resistance of HPC and compared the reinforcement corrosion characteristics of steel reinforcing bars in NC and HPC (Aïtcin 2003; El-Gelany 2001; Gowripalan and Mohamed 1998; Hansson et al. 2006; Ismail and Ohtsu 2006; Ismail and Soleymani 2002; Jaffer 2007; Lopez-Calvo et al. 2017, 2018; Nazim 2017; Presuel-Moreno et al. 2018; Soleymani and Ismail 2004; Tan 2015; Wang 2019). Gowripalan and Mohamed (1998) investigated the effectiveness of HPC in reducing the corrosion of conventional mild steel (MS) and galvanized steel. Silica fume was used to replace 10% of cement in HPC mixtures with water-cement ratios (w/c) of 0.25 and 0.35. The authors performed the rapid chloride-ion penetration test (RCPT) (ASTM C1202 2012), half-cell potential (HCP) test, and pH tests to evaluate the corrosion performance. RCPT test results showed that the charge passed through HPC at different ages (7, 28, 56, and 90 days) were much lower (0.05 to 0.5 times) than that in NC (w/c = 0.45 and 0.55), indicating that HPC reduces chloride-ion penetration significantly. HCP results showed that corrosion of both mild and galvanized steel reinforcements in NC started earlier than that in HPC. Cracking was observed in both NC and HPC after the HCP was lower than the assumed threshold of –350 mV. The findings also indicated that sufficient cover thickness was necessary for HPC, especially for structures in aggressive environments. Galvanized steel also delays the initiation of chloride-induced corrosion. Hansson et al. (2006) investigated the influence of concrete types and properties on microcell and macrocell corrosion rates. Three concrete mixtures were tested: NC (w/c = 0.43, 28-day concrete compressive strength f_c' = 41.1 MPa), HPC with 25% slag (w/b = 0.35, f_c' = 59.5 MPa), and HPC with 25% fly ash (w/b = 0.35, f_c' = 59.3 MPa). The specimens were made according to ASTM G109 (2013) and they were exposed to 2 weeks of ponding with 3% NaCl solution followed by 2 weeks of drying for 180 weeks. The linear polarization resistance (LPR) method was used to measure corrosion rates over time. It was found that the electrical resistivity of HPC was more than 5.5 times that of NC. In addition, the electrical charge passed through HPC in 6 hours per ASTM C1202 was less than 0.17 of that of NC at both 28 and 56 days. These results proved that HPC has significantly better corrosion resistance than NC. Moreover, the results of the experimental program indicated that microcell corrosion is the major mechanism of reinforcement corrosion in concrete, and that microcell corrosion is more dominant in HPC than NC due to the high resistance of HPC to ionic flow. Corrosion rate measurements showed that the macrocell corrosion rate of steel in HPC was three to four orders of magnitude lower than that in NC, while the microcell corrosion rate in HPC was just one order of magnitude lower than that in NC.

Apart from its exceptional mechanical strength, UHPC exhibits remarkable durability characteristics due to its unique composition of materials and carefully crafted mixture proportions. The dense cementitious matrix of UHPC results in low permeability, offering high resistance against moisture penetration, chloride ingress, acid exposure, carbonation, and freezing-and-thawing cycles. This has been verified through many studies that have tested the durability of UHPC made using various ingredients in various environments over the past two decades (Abbas et al. 2016; Alkaysi et al. 2016; Batoz and Behloul 2009; Ferdosian and Camões 2016; Ghafari et al. 2015; Graybeal 2005; Graybeal and Hartman 2003; Graybeal and Tanesi 2007; Pernicová 2014; Piérard et al. 2009, 2013; Shareef 2013; Sharma et al. 2018; Sritharan 2015). Graybeal and Hartman (2003), Graybeal (2005), and Graybeal and Tanesi (2007) investigated the strength and durability of UHPC mixtures (w/b = 0.15, f_c' > 186 MPa) that were cured in steam or ambient environments. The UHPC mixtures in these references were made of portland cement, silica fume, fine sand, ground quartz, high-range water-reducing admixture, and 2% (by volume) steel fibers with 0.2 mm diameter and 13 mm length. The durability investigations included chloride-ion penetration, abrasion, alkali-silica reaction (ASR), freezing-and-thawing, and scaling tests. Results of the RCPT per ASTM C1202 showed that the rapid chloride-ion permeability of all UHPC mixtures was very low or negligible and the total Coulombs passed in the tests (recorded at 1-minute intervals over the 6-hour time frame) were as low as 18 for UHPC under steam curing. Results of the chloride penetration test per AASHTO T 259 (2002) showed that the average chloride content for all mixtures was less than 0.05 kg/m^3 of concrete, which was below the minimum accuracy threshold of this test method, indicating that UHPC shows excellent resistance to chloride penetration. Results of the abrasion resistance test per ASTM C944/C944M (2012) showed that the air-cured UHPC had a higher weight loss of 1.18 to 2.1 g per abrading, while steam-cured UHPC mixtures only had 0.08 to 0.34 g per abrading. Results of the ASR test per ASTM C1260 (2014) showed that the ASR expansions of all mixtures were in the range from 0.004 to 0.023% (14 to 28 days), which was approximately an order of magnitude below the innocuous alkali-silica resistance defined by the specifications. In addition, the results of the freezing-and-thawing resistance tests per ASTM C666/C666M (2015) and scaling resistance tests per ASTM C672/C672M (2012) indicated that all UHPC mixtures had great resistance to both freezing and thawing and scaling. Based on these test results, it was concluded that UHPC mixtures exhibit superior durability, and steam-cured UHPC sections are immune to chloride-ion penetration, scaling, and freezing-and-thawing damage. Piérard et al. (2009) studied the durability and cracking of UHPC (w/b = 0.18, f_c' = 148 MPa) without fibers. The UHPC mixture was made of CEM I 42.5R cement (BS EN 197-1 2011), silica fume, quartz sand (up to 1 mm), porphyry aggregate (1 to 3 mm), and high-range water-reducing admixture. NC (w/b = 0.5, f_c' = 51 MPa) and HPC (w/b = 0.33, f_c' = 101 MPa) were also included for comparison. Two curing methods were considered: moist curing and air curing. Resistance to carbonation and chloride ingress were investigated. Accelerated carbonation test results showed that the carbonation rate of moist-cured NC, HPC, and UHPC was 0.95, 0.2, and 0.03 mm/√day respectively, while the carbonation rate of air-cured NC, HPC, and UHPC was 1.42, 0.55, and 0.06 mm/√day respectively, indicating

Table 1—Mixture proportions of concrete by weight

Concrete	Cement, Type I/II	Fly ash, Type F	Silica fume	Gravel	Fine sand	Silica sand 1	Silica sand 2	Silica powder	High-range water-reducing admixture	Water	$CaCl_2$ flakes (85%)
NC	1	—	—	2.04	2.49	—	—	—	0.0075	0.5	0.04
HPC	1	0.25	—	2.88	2.88	—	—	—	0.0125	0.56	0.04
UHPC	1	0.3	0.31	—	—	0.79	0.46	0.31	0.1	0.31	0.02

that the carbonation rate of UHPC was one order of magnitude lower than that of NC and HPC. Results of the 56-day accelerated chloride diffusion test per NT Build 443 (1995) showed that the effective chloride diffusion coefficient of moist-cured NC, HPC, and UHPC was 15.0×10^{-12}, 1.0×10^{-12}, and 0.4×10^{-12} m^2/s, respectively, while the effective chloride diffusion coefficient of air-cured NC, HPC, and UHPC was 22.2×10^{-12}, 2.1×10^{-12}, and 0.4×10^{-12} m^2/s, respectively, indicating that UHPC has considerably better chloride diffusion resistance than NC and HPC. In addition, the authors investigated the cracking tendency of UHPC under restrained conditions by performing shrinkage measurements and ring tests. The results of these tests showed that UHPC has higher autogenous shrinkage, which potentially could lead to cracking. The authors also indicated that by adding steel fibers to UHPC mixtures, resistance of UHPC to microcracks caused by restricted shrinkage can be improved.

Despite previous studies having demonstrated the improved durability and corrosion resistance of HPC and UHPC, as well as that of corrosion-resistant reinforcing steels, there remains a lack of a systematic study of the corrosion behavior of different types of reinforcements in different types of concrete. This study aims to directly compare the corrosion performance of various reinforcements, including conventional MS, EC, HC, and SS steel, when embedded in different types of concretes, including NC, HPC, and UHPC.

RESEARCH SIGNIFICANCE

The corrosion of steel reinforcement in RC structures has been a major issue globally. To address this, two practical solutions are the use of more durable concretes and corrosion-resistant reinforcements. This study directly compares the corrosion resistance of various reinforcements, including conventional MS, EC, HC, and SS steel, in different types of concretes (NC, HPC, and UHPC) for large-scale specimens in circular column configuration. The results from this research are expected to promote the wider use of corrosion-resistant reinforcements and more durable concretes, leading to the creation of more sustainable and long-lasting civil infrastructure.

EXPERIMENTAL INVESTIGATION

The corrosion resistance of four commonly used reinforcements—MS, EC, HC, and SS steel—were investigated in three different types of concrete with varying levels of strength and durability—that is, NC, HPC, and UHPC. MS reinforcement in NC was used as a reference for comparison. Circular columns with both longitudinal and transverse

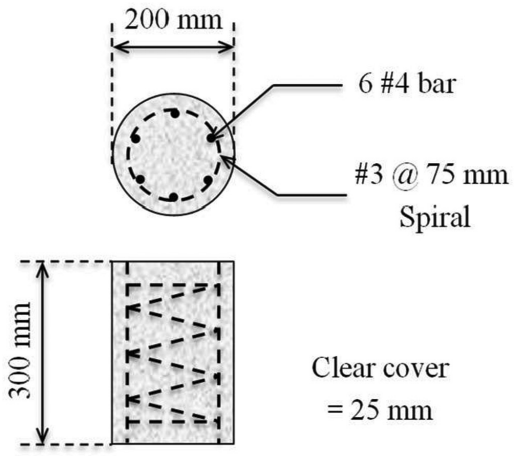

Fig. 1—Schematic of column specimens.

reinforcements were used to simulate real RC structures. The HCP, LPR, and electrochemical impedance spectroscopy (EIS) were used to assess the corrosion activity and corrosion rate, along with direct reinforcement mass loss measurements of the corroded reinforcements after accelerated aging exposure.

Materials

The proportions of the concrete mixtures are presented in Table 1. The compressive strengths at 28 days for NC, HPC, and UHPC were 42.7, 69.6, and 150 MPa, respectively. In this study, $CaCl_2$ flakes were added to the concrete mixtures directly during mixing to accelerate the corrosion process. The four types of reinforcement studied were ASTM A615/A615M Grade 60 conventional MS reinforcement, ASTM A775/A775M Grade 60 EC reinforcement, ASTM A1035/A1035M Grade 100 HC steel reinforcement, and ASTM A995/A995M Grade 75 SS reinforcement (Type 2304 SS). The chemical compositions of these reinforcements are given in Tables 2 and 3.

Specimens

Column specimens, as shown in Fig. 1, were selected in this experimental program to imitate real-life RC structures. Different combinations of three different types of concrete and four types of reinforcements were investigated in the experimental program, as shown in Table 4. A volumetric transverse reinforcement ratio of 2.45% and six longitudinal bars were used to ensure the column specimen with traditional materials (NC+MS) complies with ACI 318-19 recommendations (ACI Committee 318 2019). The reinforcement arrangement in all column specimens was identical to eliminate any impact on corrosion behavior. A total

Table 2—Chemical composition of transverse steel reinforcing bars

Element, wt. %	C	Mn	P	S	Si	Cu	Ni	Cr
MS	0.410	0.800	0.012	0.029	0.210	0.290	0.200	0.170
EC	0.440	0.630	0.009	0.050	0.180	0.360	0.140	0.140
HC	0.100	0.670	0.008	0.010	0.390	0.110	0.080	9.81
SS	0.016	1.500	0.031	0.0003	0.570	0.270	4.230	22.58
Element, wt. %	V	Mo	Sn	N	Cb	Co	Al	CE
MS	0.002	0.041	0.008	—	—	—	0.002	—
EC	—	0.034	0.011	—	0.001	—	0.001	—
HC	0.020	0.020	0.008	0.012	—	—	—	1.200
SS	—	0.180	—	0.128	—	0.080	—	—

Table 3—Chemical composition of longitudinal steel reinforcing bars

Element, wt. %	C	Mn	P	S	Si	Cu	Ni	Cr
MS	0.370	0.970	0.014	0.019	0.210	0.320	0.180	0.220
EC	0.430	0.790	0.014	0.037	0.180	0.360	0.130	0.170
HC	0.110	0.640	0.007	0.009	0.300	0.150	0.100	9.71
SS	0.017	1.800	0.030	0.0009	0.470	0.240	3.740	22.58
Element, wt. %	V	Mo	Sn	N	Cb	Co	Al	CE
MS	0.004	0.039	—	—	—	—	—	—
EC	0.001	0.046	0.010	—	0.002	—	0.002	—
HC	0.020	0.020	0.011	0.013	—	—	—	1.190
SS	—	0.270	—	0.166	—	0.100	—	—

Table 4—Test matrix

Conc. \ Reinf.	MS	EC	HC	SS
NC	Two specimens—exposure of 12 and 24 months, respectively, for each concrete and reinforcement combination			
HPC				
UHPC				

of 24 specimens were made and subjected to aggressive environmental exposure for up to 24 months to evaluate the corrosion performance of the reinforcements and measure the mass loss due to corrosion. The initial weight of each longitudinal and transverse reinforcing bar was recorded and then secured in a cage for concrete casting. Plastic ties, rather than steel wires, were used to tie the longitudinal and transverse bars, avoiding any influence on reinforcement corrosion. Copper wires were connected to both the longitudinal and transverse reinforcements for electrochemical corrosion rate measurements, and the connection areas were sealed with electrical tape.

Test procedures

First, column specimens were fabricated at a concrete plant. After a 28-day curing period in ambient environment, all specimens were put into an aggressive environment (refer to the next section) for 12 months. Once the first 12 months of exposure were completed, the reinforcing bars were carefully extracted from the columns to avoid damaging the bars. These reinforcing bars were then cleaned according to ASTM G1 (2003), and the mass loss was measured. The remaining 12 specimens were kept in the accelerated environment for an additional 12 months. After 24 months of exposure, the reinforcing bars were extracted in a similar way, and the mass loss was measured and recorded.

Environmental conditions

In this study, the process of corrosion was accelerated by immersing the concrete columns in a heated 5% (wt. %) chloride solution for 9 months. The temperature was maintained at 40°C. The solution was drained and the specimens were allowed to dry for 2 days in every 4-day cycle. Starting from the tenth month, the wetting-and-drying cycle was increased to every 4 hours (2 hours wet, 2 hours dry) to further increase the rate of corrosion.

Electrochemical corrosion measurements

The corrosion of reinforcement in the columns was monitored using a potentiostat. Three corrosion evaluation techniques were used: HCP, LPR, and EIS. HCP tests were used to assess the initiation of corrosion, while the LPR tests were used to measure corrosion rates of MS, HC, and SS reinforcements. EIS tests were used to measure the corrosion rate of EC due to the limitation of LPR. Figure 2 illustrates the three electrodes necessary for LPR and EIS tests. In the test setup, reinforcing bars within the column served as the working electrodes (WE), with a copper/copper sulfate reference electrode (RE) probe acting as the RE and placed on top of the concrete through a wet sponge to maintain an electrical connection. A titanium mesh surrounding the surface of the columns was used as the counter electrode

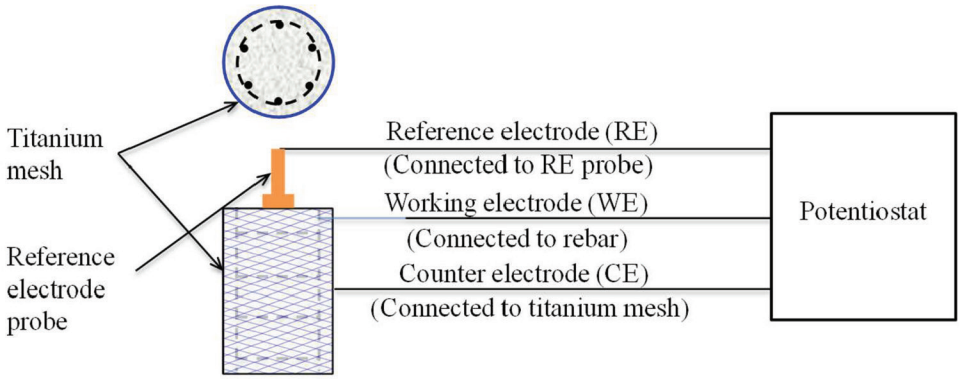

Fig. 2—Schematic of LPR/EIS test setups.

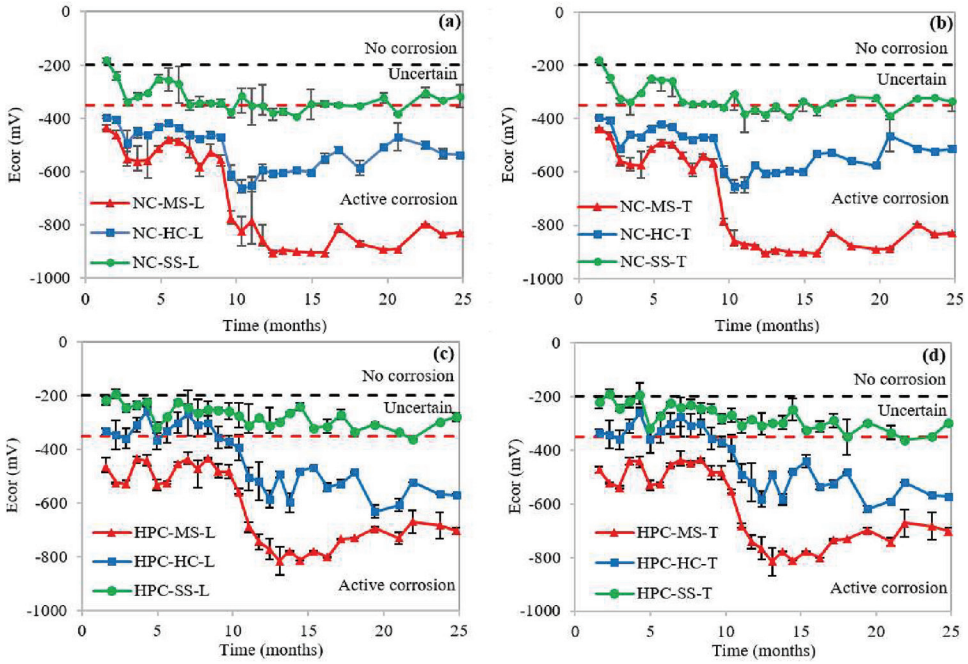

Fig. 3—HCP measurements of reinforcements in columns: (a) NC longitudinal; (b) NC transverse; (c) HPC longitudinal; and (d) HPC transverse reinforcement.

(CE), with an electrical connection maintained by a damp cloth between the titanium mesh and the column surface.

EXPERIMENTAL RESULTS AND DISCUSSION

Half-cell potential

The HCP results of MS, HC, and SS in the NC, HPC, and UHPC columns are presented in Fig 3. The data shown in the figure are the average of four readings taken from two columns and two readings from different locations of one column during 2 to 13 months and 14 to 25 months, respectively. The vertical error bars in the figure indicate the range of the minimum and maximum values among all the readings at a given time. The x-axis represents the time in months and the y-axis represents the HCP relative to the reference electrode. The dashed lines in the figure divide the "no corrosion," "uncertain," and "active corrosion" zones according to ASTM C876 (2015), with values of –200 and –350 mV, respectively.

It is seen in Fig. 3 that in both NC and HPC columns, the HCP values from high to low follow the order of SS, HC, and MS, indicating the order of corrosion activity from low to high. The HCP values of MS and HC were always below –350 mV and in the "active corrosion" region, indicating that NC and even HPC were not able to provide adequate protection to the reinforcement under the aggressive environmental conditions of this study. Furthermore, the HCP values of MS and HC decreased significantly in the ninth month and remained relatively stable thereafter, indicating significant corrosion activity between 10 and 25 months. Additionally, no significant differences in HCP values were observed between the longitudinal and transverse reinforcements in both NC and HPC columns. For SS, the HCP values were always close to or higher than –350 mV, indicating a very minor possibility of active corrosion.

The HCP values for MS, HC, and SS in the UHPC columns were consistently above –350 mV, indicating a low likelihood of active corrosion. This demonstrates that UHPC provides exceptional durability and effectively protects the reinforcement from corrosion.

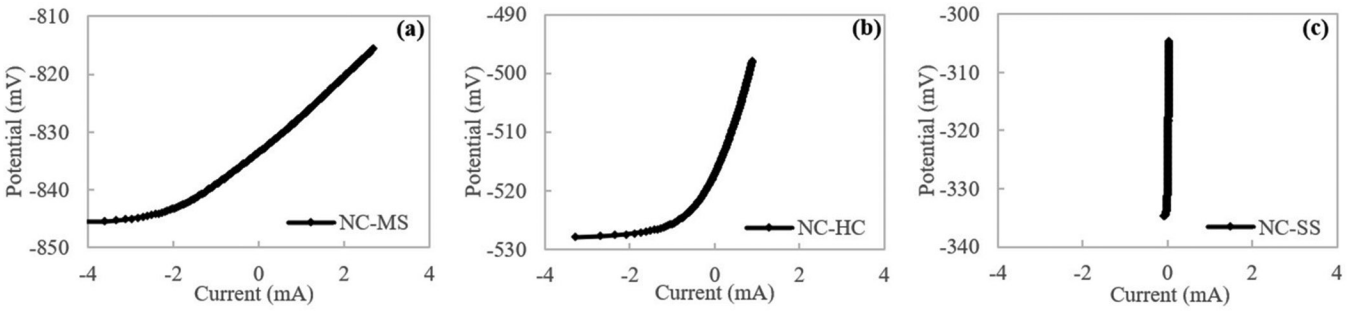

Fig. 4—LPR plot examples of reinforcement in NC at 24 months of exposure: (a) MS; (b) HC; and (c) SS.

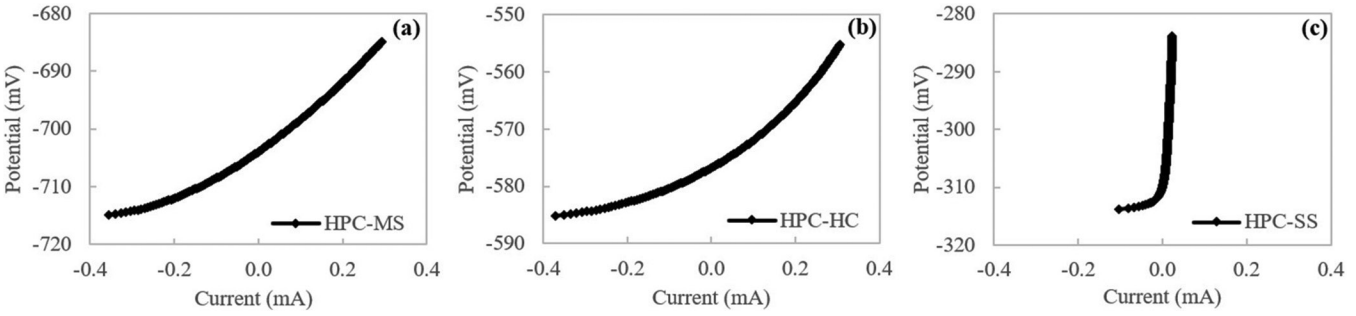

Fig. 5—LPR plot examples of reinforcement in HPC at 24 months of exposure: (a) MS; (b) HC; and (c) SS.

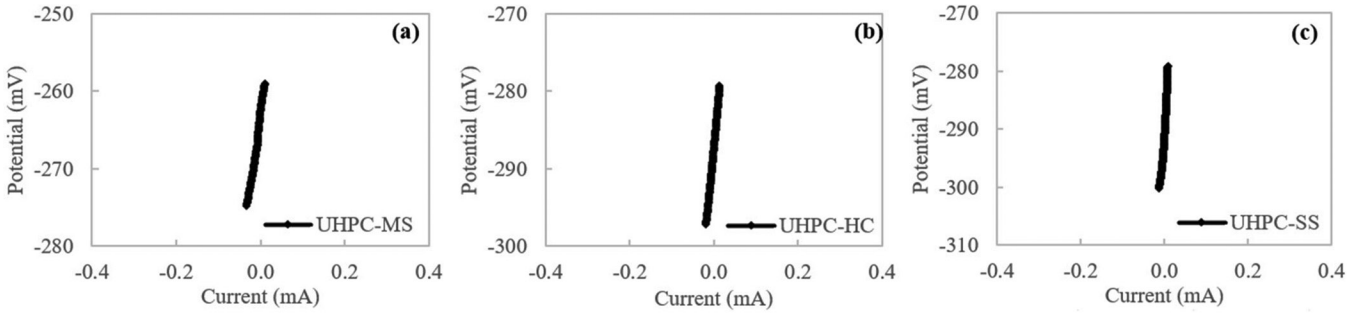

Fig. 6—LPR plot examples of reinforcement in UHPC at 24 months of exposure: (a) MS; (b) HC; and (c) SS.

Corrosion rate

The corrosion rates of bare reinforcement were determined using LPR tests. Figures 4, 5, and 6 show the representative LPR plots of MS, HC, and SS in NC, HPC, and UHPC columns, respectively, after 24 months of accelerated aging exposure. In the plots, the x-axis represents the corrosion current and the y-axis represents the corrosion potential relative to the copper/copper sulfate RE. The slope of the LPR curves near the corrosion potential (where the corrosion current is zero) indicates the polarization resistance. Figure 4 demonstrates that in NC columns, the MS curve has the smallest slope, while the SS curve has the largest slope among the three curves, indicating that the polarization resistance from large to small follows the order of SS, HC, and MS. In HPC columns, as shown in Fig. 5, the slopes of the MS and HC LPR plots are similar, while the slope of the SS curve is much larger, meaning that SS has a much higher polarization resistance than MS and HC, and MS and HC have close polarization resistances. In the UHPC columns, as shown in Fig. 6, all slopes were very large and the polarization resistances were very high, indicating negligible corrosion rates.

The corrosion rate of the EC reinforcement was determined using the EIS tests. Figure 7 presents an example of the EIS plot of EC in both NC and HPC. The Nyquist plot, as depicted in Fig. 7(a), has the real part of the impedance (Z_{real}) on the x-axis and the imaginary part of the impedance (Z_{img}) on the y-axis. The magnitude of the impedance ($|Z|$) is represented by the distance between the plotted point and the origin, and the slope of the line connecting the plotted point to the origin represents the phase shift (Φ). In the Bode plot, shown in Fig. 7(b), the x-axis is the applied alternating current (AC) frequency (w), the magnitude of the impedance ($|Z|$) is on the left y-axis, and the phase shift (Φ) is on the right y-axis. The electrical equivalent circuit (EEC) shown in Fig. 8 was used to fit the EIS data in this study. The EEC includes the resistance of the concrete (R_s), the resistance and capacitance of the epoxy-coating pores (R_c and CPE_c), the resistance and capacitance of the film on the reinforcement surface (R_{layer} and CPE_{layer}), the capacitance of the double layer (CPE_{dl}), and the polarization resistance (R_{ct}). It should be noted that in the concrete-reinforcement system, the coating capacitance, film capacitance, and electric double-layer capacitance often deviate from pure capacitance due to

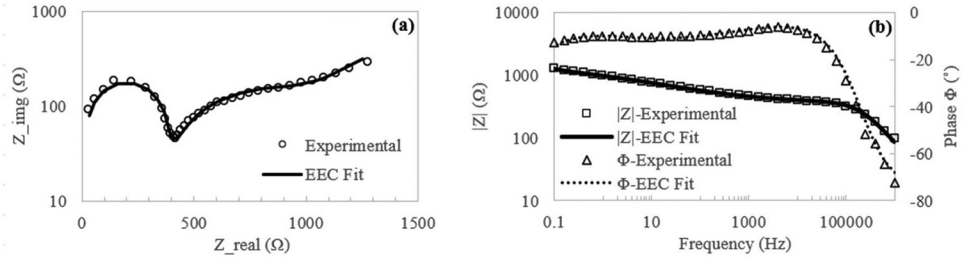

Fig. 7—EIS data fitting example of EC in: (a) Nyquist plot; and (b) Bode plot.

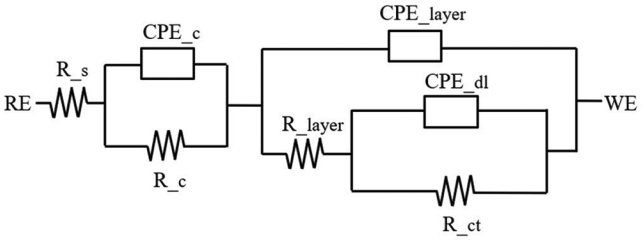

Fig. 8—Electrical equivalent circuit used in EIS fitting.

the dispersion effect. As a result, the constant phase element (CPE) was used in the EEC model instead of pure capacitance. The results of the fitting showed that the proposed EEC fits the experimental data well, as illustrated in Fig. 7.

Once the polarization resistances were obtained, the corrosion rate of the reinforcement was determined according to ASTM G102 (1989). The results are shown in Fig. 9, which summarizes the corrosion rates obtained from LPR tests on MS, HC, and SS in NC and HPC columns. The average corrosion rate values displayed in the figure are based on the average of four measurements on two columns and two measurements on one column during 2 to 13 months and 14 to 25 months, respectively. The error bars in the figure indicate the range between the minimum and maximum values among all the measurements taken at a certain time. On the x-axis, the time is measured in months, while the y-axis represents the corrosion rate in mils per year (mpy). The dashed lines in the figure correspond to the dividing values for low, moderate, and high corrosion rates according to Cady and Gannon (1993) and Ji (2005) with values of 0.046, 0.228, and 0.456 mpy, respectively.

As seen in Fig. 9, MS in NC columns underwent severe corrosion in the accelerated aging environment. The first measurement of the corrosion rate at the end of the first month was approximately 0.5 mpy, and by the end of the 24-month exposure, the rate had increased fourfold to over 2 mpy. The maximum corrosion rate recorded during the entire period was 2.9 mpy. Meanwhile, HC reinforcements showed similar corrosion rates before the seventh month but then significantly decreased. After the 12th month, the corrosion rates of HC were less than half those of MS. On the other hand, the corrosion rates of SS reinforcements were negligible throughout the entire exposure period. Additionally, it was discovered that the transverse reinforcements of MS and HC experienced slightly higher corrosion rates than the longitudinal reinforcements. This is because the transverse reinforcements were closer to the concrete cover and had better access to moisture, oxygen, and the accelerated corrosion environment. Furthermore, as shown in Fig. 10, more corrosion was observed on the outer surface of the transverse reinforcements for the same reason.

In HPC columns, both MS and HC reinforcements showed low to moderate corrosion rates, with values less than 0.5 mpy at all times. These rates were significantly lower than those of MS and HC in NC columns, indicating the better protection provided by HPC. There was no significant difference between the corrosion rates of MS and HC throughout the entire accelerated aging exposure, which may be due to the protection of HPC making the controlling factor for corrosion the access to moisture and oxygen, rather than the reinforcement's corrosion resistance. Additionally, longitudinal and transverse reinforcements showed similar corrosion rates in HPC due to the overall low corrosion rates of the reinforcements well-protected by HPC cover. The corrosion rates of SS reinforcements remained negligible throughout the entire period, as they did in NC.

In NC and HPC columns, the EIS tests revealed that the EC reinforcements had negligible corrosion rates, owing to the effective protection provided by the epoxy coating that prevented the steel reinforcements from being exposed to moisture and oxygen, which are the essential elements for corrosion. Additionally, throughout the entire exposure period, the corrosion rates of all four types of reinforcements in UHPC columns were always negligible, as the high packing density of the UHPC effectively inhibited the diffusion of oxygen and moisture, which are crucial factors for corrosion.

In summary, the results of the electrochemical corrosion rate measurements demonstrated that none of the EC and SS reinforcements in NC and HPC, and all the reinforcements in UHPC showed signs of corrosion during the 24-month accelerated corrosion exposure. The corrosion rates of MS and HC in NC were much higher compared to the same reinforcement types in HPC during the same measurement periods. On average, the corrosion rate of MS and HC in NC was 6.6 and 2.8 times, respectively, that of the same reinforcement types in HPC over the 24-month exposure period. UHPC showed the best corrosion resistance, followed by HPC, while NC exhibited the weakest performance. Additionally, the results showed that MS had a higher corrosion rate than HC in NC, with the average corrosion rate of MS being twice that of HC. However, in HPC, the average corrosion rates of MS and HC were almost the same, likely due to limited access to oxygen and moisture.

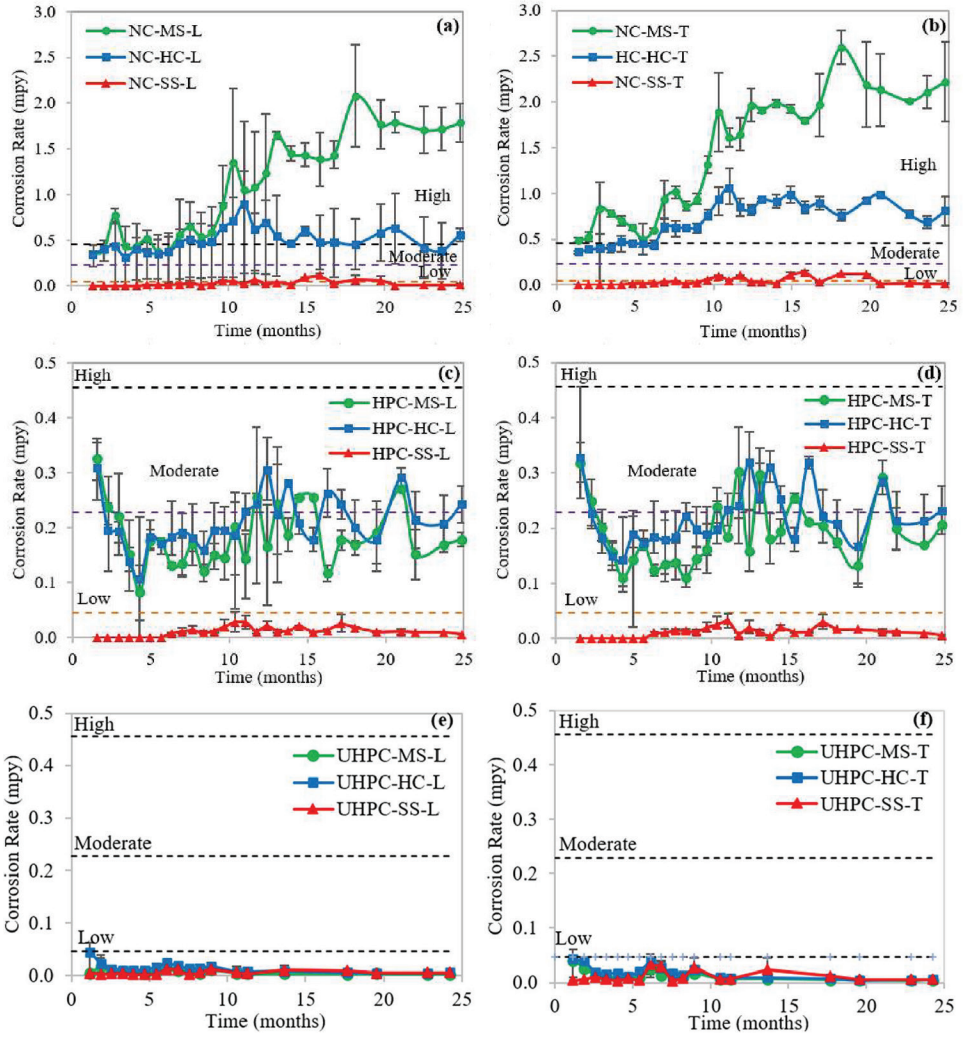

Fig. 9—LPR corrosion rates of reinforcement in columns: (a) NC longitudinal; (b) NC transverse; (c) HPC longitudinal; (d) HPC transverse; (e) UHPC longitudinal; and (f) UHPC transverse reinforcement.

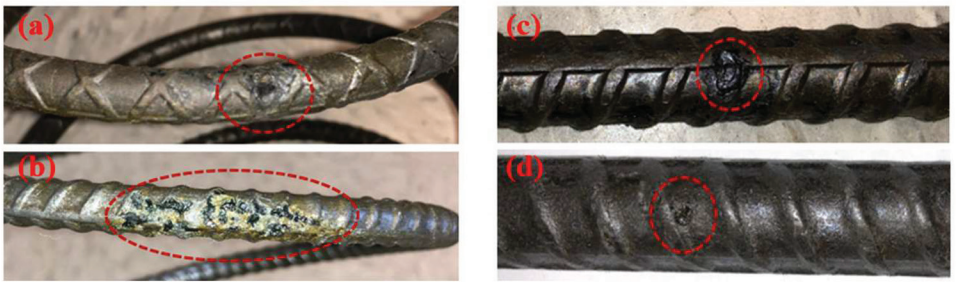

Fig. 10—Examples of pitting corrosion of reinforcement in HPC: (a) MS transverse; (b) HC transverse; (c) MS longitudinal; and (d) HC longitudinal reinforcement.

Reinforcement mass loss

At the end of 12 and 24 months of exposure, the reinforcing bars were carefully removed from the column specimens to prevent damage. These reinforcing bars were then cleaned according to ASTM G1, and the mass loss was measured. As depicted in Fig. 10, MS and HC in HPC columns also exhibited signs of pitting corrosion. Moreover, corrosion was evident only on one side of the reinforcing bars, the side facing the cover concrete, which was closer to the aggressive environment.

The results of the mass loss measurements of the column specimens after 12 and 24 months of accelerated corrosion exposure are presented in Fig. 11. The results showed negligible mass loss for EC and SS reinforcements, indicating that they remained free of corrosion even after 24 months of exposure to the aggressive environment. On the other hand, loss of mass was observed in MS and HC reinforcements. The mass losses of MS, both longitudinal and transverse reinforcements, were found to be higher than those of HC: the mass losses of HC were 44 to 54% (with an average of 47%) and 64 to 82% (with an average of 75%) of that

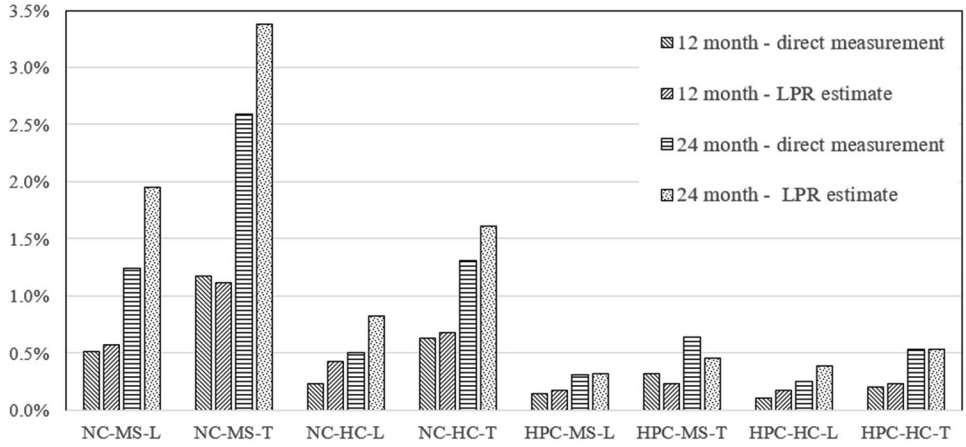

Fig. 11—Reinforcement mass loss in NC and HPC columns. (Note: L and T, respectively, indicate longitudinal and transverse reinforcement.)

of MS in NC and HPC columns, respectively. The results also indicated that the mass losses of MS and HC in NC after 24 months of exposure were 4.0 and 2.3 times, respectively, that of MS and HC in HPC. This can be attributed to the protection offered by HPC against the penetration of oxygen and moisture. The results also showed that the mass loss of transverse reinforcements were higher than those of longitudinal reinforcements, with the average mass loss of transverse reinforcements being 2.3 and 2.1 times that of longitudinal reinforcements in NC and HPC, respectively, due to the easier access of moisture and oxygen to transverse reinforcement. Finally, the findings indicated that the mass losses in the second 12 months (months 13 to 25) were slightly higher than twice those of the first 12 months (months 1 to 13), suggesting that corrosion in the second 12 months was more active than in the first 12 months. For UHPC specimens, no mass loss was observed in any of the four types of reinforcements, owing to the excellent protection offered by the UHPC cover, which has been demonstrated to have the highest durability.

The results from the mass loss measurements were compared with the mass loss estimations obtained from the electrochemical corrosion rate measurements using Faraday's law, which is expressed as

$$m = \frac{M \cdot I \cdot t}{n \cdot F} \quad (1)$$

where m is the mass loss of steel in grams; M is the atomic weight, which is 55.85 g/mol for iron; I is the current in amperes; t is the time in seconds; n is the number of valence electrons, which is 2 for iron; and F is Faraday's constant, which is 96,487 coulombs/mol.

Figure 11 presents the calculated mass loss from electrochemical corrosion rate measurements for the NC and HPC columns. There are differences between the mass loss directly measured from columns and the ones estimated from electrochemical measurements; the directly measured mass loss was 54 to 106% (with an average of 78%) and 60 to 142% (with an average of 97%) of the estimated mass loss in NC and HPC columns, respectively. The differences are attributed to three reasons. First, the directly measured mass loss reflected the total impact of corrosion activities over the entire exposure period, while the estimated mass loss only represented the corrosion activities at the moment the corrosion rate measurements were taken. Second, it was noted that electrochemical methods may overestimate the corrosion rate (Alghamdi and Ahmad 2014; Zou et al. 2011). Alghamdi and Ahmad (2014) reported that the gravimetrically measured corrosion rate was on average 86% of the electrochemically measured rate, which agrees with the findings here. Lastly, corrosion activity may vary greatly in different parts of the same column and in different reinforcements in different columns.

CONCLUSIONS

An experimental study that directly compares the corrosion behavior of mild steel (MS), epoxy-coated steel (EC), high-chromium steel (HC), and stainless steel (SS) in normal-strength concrete (NC), high-performance concrete (HPC), and ultra-high-performance concrete (UHPC) in a chloride environment was performed. The research findings led to the following main conclusions:

1. UHPC proved to be highly durable, protecting the embedded reinforcements from any corrosion activity even after 24 months of accelerated corrosion exposure. HPC was also found to be more durable than NC, with the mass loss of MS and HC in HPC being 25 to 49% of that in NC.

2. EC and SS showed negligible mass loss even after 24 months in an aggressive environment.

3. HC was found to have better corrosion resistance than MS in NC. Based on the measurements after 24 months of exposure, the average corrosion rates of HC were 50% and 75% of that of MS in NC and HPC, respectively.

4. Transverse reinforcing bars were more susceptible to corrosion than longitudinal reinforcing bars, due to their higher exposure to chloride, moisture, and oxygen. Mass loss measurements revealed that the corrosion rates of longitudinal reinforcements were 48%, 39%, 49%, and 47% of those of transverse reinforcements for MS in NC, HC in NC, MS in HPC, and HC in HPC, respectively, after 24 months of accelerated aging exposure.

5. Pitting corrosion was found to dominate MS and HC in NC and HPC under a chloride attack environment.

6. Half-cell potential (HCP) was found to be a reliable indicator of corrosion activity, with results for MS, HC, SS reinforcements in all three types of concrete agreeing with the mass loss measurements.

7. Linear polarization resistance (LPR) tests were found to potentially overestimate corrosion activity. Results showed that the mass losses directly measured from columns were 78% and 97% of that estimated from the electrochemical corrosion rate measurements in NC and HPC, respectively. It is noted that the mass loss measured directly from the reinforcements in columns represents the cumulative mass loss over 24 months of exposure, while the mass loss estimated from electrochemical corrosion rate measurements only represent the instantaneous corrosion status at the time when these measurements were taken.

AUTHOR BIOS

Ben Wang *is a Researcher at the University of Houston, Houston, TX, where he received his PhD in civil engineering. He received his BS and MS from Tongji University, Shanghai, China. His research interests include high-performance concrete (HPC), ultra-high-performance concrete (UHPC), corrosion-resistant reinforcement, durability of reinforced concrete, service life prediction, and life-cycle cost analysis of reinforced concrete structures.*

Abdeldjelil Belarbi, *FACI, is a Hugh Roy and Lillie Cranz Cullen Distinguished Professor at the University of Houston. He is the current Chair of the ACI Technical Activities Committee's Subcommittee on ACI/ASCE-SEI Joint Committees; past Chair of Joint ACI-ASCE Committee 445, Shear and Torsion, and ACI Subcommittee 440-E, FRP-Prof Education; and a member of ACI Committees 341, Performance-Based Seismic Design of Concrete Bridges, and 440, Fiber-Reinforced Polymer Reinforcement; and ACI Subcommittee 318-E, Section and Member Strength. His research interests include constitutive modeling, analytical and experimental investigations of reinforced and prestressed concrete structures, as well as the use of advanced materials for new construction and rehabilitation of existing infrastructure.*

Mina Dawood *is an Associate Professor at the University of Houston and an Associate Editor of the ASCE* Journal of Composites for Construction. *His research interests include the development and implementation of new materials, systems, and techniques in structural applications for both repair/rehabilitation and new construction.*

Bora Gencturk *is an Associate Professor in the Sonny Astani Department of Civil and Environmental Engineering and the Director of the Structures and Materials Research Laboratory at the University of Southern California, Los Angeles, CA. Gencturk is a member of ACI Committees 341, Performance-Based Seismic Design of Concrete Bridges, and 440, Fiber-Reinforced Polymer Reinforcement. His research interests include the durability and extreme event resilience of reinforced concrete structures with an emphasis on application of high-performance materials.*

ACKNOWLEDGMENTS

The funding for this research was provided by the National Priorities Research Program of the Qatar National Research Fund (a member of the Qatar Foundation) under award No. NPRP 7-410-2-169. The statements made herein are solely the responsibility of the authors and do not necessarily reflect the opinions of the sponsor.

REFERENCES

AASHTO T 259, 2002, "Standard Method of Test for Resistance of Concrete to Chloride Ion Penetration," American Association of State Highway and Transportation Officials, Washington, DC.

Abbas, S.; Nehdi, M. L.; and Saleem, M. A., 2016, "Ultra-High Performance Concrete: Mechanical Performance, Durability, Sustainability and Implementation Challenges," *International Journal of Concrete Structures and Materials*, V. 10, No. 3, pp. 271-295. doi: 10.1007/s40069-016-0157-4

ACI Committee 222, 2001, "Protection of Metals in Concrete Against Corrosion (ACI 222R-01)," American Concrete Institute, Farmington Hills, MI, 41 pp.

ACI Committee 318, 2019, "Building Code Requirements for Structural Concrete (ACI 318-19) and Commentary (ACI 318R-19) (Reapproved 2022)," American Concrete Institute, Farmington Hills, MI, 625 pp.

ACI Committee 363, 2010, "Report on High-Strength Concrete (ACI 363R-10)," American Concrete Institute, Farmington Hills, MI, 65 pp.

Aïtcin, P. C., 2003, "The Durability Characteristics of High-Performance Concrete: A Review," *Cement and Concrete Composites*, V. 25, No. 4-5, pp. 409-420. doi: 10.1016/S0958-9465(02)00081-1

Alghamdi, S. A., and Ahmad, S., 2014, "Service Life Prediction of RC Structures Based On Correlation Between Electrochemical and Gravimetric Reinforcement Corrosion Rates," *Cement and Concrete Composites*, V. 47, pp. 64-68. doi: 10.1016/j.cemconcomp.2013.06.003

Alkaysi, M.; El-Tawil, S.; Liu, Z.; and Hansen, W., 2016, "Effects of Silica Powder and Cement Type On Durability of Ultra High Performance Concrete (UHPC)," *Cement and Concrete Composites*, V. 66, pp. 47-56. doi: 10.1016/j.cemconcomp.2015.11.005

ASTM C666/C666M-15, 2015, "Standard Test Method for Resistance of Concrete to Rapid Freezing and Thawing," ASTM International, West Conshohocken, PA.

ASTM C672/C672M-12, 2012, "Standard Test Method for Scaling Resistance of Concrete Surfaces Exposed to Deicing Chemicals," ASTM International, West Conshohocken, PA.

ASTM C876-15, 2015, "Standard Test Method for Corrosion Potentials of Uncoated Reinforcing Steel in Concrete," ASTM International, West Conshohocken, PA.

ASTM C944/C944M-12, 2012, "Standard Test Method for Abrasion Resistance of Concrete or Mortar Surfaces by the Rotating-Cutter Method," ASTM International, West Conshohocken, PA.

ASTM C1202-12, 2012, "Standard Test Method for Electrical Indication of Concrete's Ability to Resist Chloride Ion Penetration," ASTM International, West Conshohocken, PA.

ASTM C1260-14, 2014, "Standard Test Method for Potential Alkali Reactivity of Aggregates," ASTM International, West Conshohocken, PA.

ASTM G1-03(2011), 2003, "Standard Practice for Preparing, Cleaning, and Evaluating Corrosion Test," ASTM International, West Conshohocken, PA.

ASTM G102-89(2010), 1989, "Standard Practice for Calculation of Corrosion Rates and Related Information from Electrochemical Measurements," ASTM International, West Conshohocken, PA.

ASTM G109-13, 2013, "Standard Test Method for Determining the Effects of Chemical Admixtures on the Corrosion of Embedded Steel Reinforcement in Concrete Exposed to Chloride Environments," ASTM International, West Conshohocken, PA.

Batoz, J., and Behloul, M., 2009, "UHPFRC Development on the Last Two Decades: An Overview," *UHPFRC Conference*, Marseille, France, pp. 1-13.

BS EN 197-1:2011, 2011, "Cement - Composition, Specifications and Conformity Criteria for Common Cements," British Standards Institution, London, UK.

Cady, P. D., and Gannon, E. J., 1993, "Condition Evaluation of Concrete Bridges Relative to Reinforcement Corrosion, Volume 8: Procedure Manual," *SHRP-S-330*, Strategic Highway Research Program, Washington, DC.

Cui, F., 2003, "Corrosion Behavior of Stainless Steel Clad Rebar," PhD dissertation, University of South Florida, Tampa, FL.

Darwin, D.; O'Reilly, M.; Somogie, I.; Sperry, J.; Lafikes, J.; Storm, S.; and Browning, J., 2013, "Stainless Steel Reinforcement as a Replacement for Epoxy Coated Steel in Bridge Decks," Report FHWA-OK-13-08, University of Kansas Center for Research, Inc., Lawrence, KS.

El-Gelany, M., 2001, "Short-Term Corrosion Rate Measurement of NC and HPC Reinforced Concrete Specimens by Electrochemical Techniques," *Materials and Structures*, V. 34, No. 7, pp. 426-432. doi: 10.1007/BF02482289

Ferdosian, I., and Camões, A., 2016, "Ultra-High Durable Concrete: A Way Towards Safe and Durable Structures," *7th International Conference on Safety and Durability of Structures (ICOSADOS 2016)*, Vila Real, Portugal.

Ghafari, E.; Arezoumandi, M.; Costa, H.; and Júlio, E., 2015, "Influence of Nano-Silica Addition in the Durability of UHPC," *Construction and Building Materials*, V. 94, pp. 181-188. doi: 10.1016/j.conbuildmat.2015.07.009

Gowripalan, N., and Mohamed, H. M., 1998, "Chloride-Ion Induced Corrosion of Galvanized and Ordinary Steel Reinforcement in High-Performance Concrete," *Cement and Concrete Research*, V. 28, No. 8, pp. 1119-1131. doi: 10.1016/S0008-8846(98)00090-8

Graybeal, B., 2005, "Characterization of the Behavior of Ultra-High-Performance Concrete," PhD dissertation, University of Maryland, College Park, MD.

Graybeal, B., 2006, "Material Property Characterization of Ultra-High Performance Concrete," Report No. FHWA-HRT-06-103, Federal Highway Administration, McLean, VA.

Graybeal, B., and Hartman, J., 2003, "Strength and Durability of Ultra-High Performance Concrete," *Concrete Bridge Conference*, pp. 1-20

Graybeal, B., and Tanesi, J., 2007, "Durability of an Ultrahigh-Performance Concrete," *Journal of Materials in Civil Engineering*, ASCE, V. 19, No. 10, pp. 848-854. doi: 10.1061/(ASCE)0899-1561(2007)19:10(848)

Hansson, C. M.; Poursaee, A.; and Jaffer, S. J., 2007, "Corrosion of Reinforcing Bars in Concrete," *R&D Serial No. 3013*, Portland Cement Association, Skokie, IL.

Hansson, C. M.; Poursaee, A.; and Laurent, A., 2006, "Macrocell and Microcell Corrosion of Steel in Ordinary Portland Cement and High Performance Concretes," *Cement and Concrete Research*, V. 36, No. 11, pp. 2098-2102. doi: 10.1016/j.cemconres.2006.07.005

Ismail, M., and Ohtsu, M., 2006, "Corrosion Rate of Ordinary and High-Performance Concrete Subjected to Chloride Attack by AC Impedance Spectroscopy," *Construction and Building Materials*, V. 20, No. 7, pp. 458-469. doi: 10.1016/j.conbuildmat.2005.01.062

Ismail, M., and Soleymani, H. R., 2002, "Monitoring Corrosion Rate for Ordinary Portland Concrete (NC) And High-Performance Concrete (HPC) Specimens Subjected to Chloride Attack," *Canadian Journal of Civil Engineering*, V. 29, No. 6, pp. 863-874. doi: 10.1139/l02-091

Jaffer, S. J., 2007, "The Influence of Loading on the Corrosion of Steel in Cracked Ordinary Portland Cement and High Performance Concretes," PhD thesis, University of Waterloo, Waterloo, ON, Canada.

Ji, J., 2005, "Corrosion Resistance of Microcomposite and Duplex Stainless Steels for Reinforced Concrete Bridge Decks," PhD dissertation, University of Kansas, Lawrence, KS.

Lopez-Calvo, H. Z.; Montes-Garcia, P.; Alonso-Guzmán, E. M.; Martinez-Molina, W.; Bremner, T. W.; and Thomas, M. D. A., 2017, "Effects of Corrosion Inhibiting Admixtures and Supplementary Cementitious Materials Combinations On the Strength and Certain Durability Properties of HPC," *Canadian Journal of Civil Engineering*, V. 44, No. 11, pp. 918-926. doi: 10.1139/cjce-2016-0237

Lopez-Calvo, H. Z.; Montes-García, P.; Jiménez-Quero, V. G.; Gómez-Barranco, H.; Bremner, T. W.; and Thomas, M. D. A., 2018, "Influence of Crack Width, Cover Depth and Concrete Quality On Corrosion of Steel in HPC Containing Corrosion Inhibiting Admixtures and Fly Ash," *Cement and Concrete Composites*, V. 88, pp. 200-210. doi: 10.1016/j.cemconcomp.2018.01.016

Nazim, M., 2017, "Corrosion Propagation of Rebar Embedded in High Performance Concrete," master's thesis, Florida Atlantic University, Boca Raton, FL.

NT Build 443, 1995, "Concrete, Hardened: Accelerated Chloride Penetration," NORDTEST, Oslo, Norway.

Pernicová, R., 2014, "Chloride Transport in Ultra High Performance Concrete," *International Journal of Materials and Metallurgical Engineering*, V. 8, No. 11, pp. 1060-1063.

Piérard, J.; Cauberg, N.; and Remy, O., 2009, "Evaluation of Durability and Cracking Tendency of Ultra High-Performance Concrete," *Proceedings, 8th International Conference on Creep, Shrinkage and Durability Mechanics of Concrete and Concrete Structures (CONCREEP 8)*, Ise-Shima, Japan, pp. 695-700.

Piérard, J.; Dooms, B.; and Cauberg, N., 2013, "Durability Evaluation of Different Types of UHPC," *RILEM*-fib-*AFGC International Symposium on Ultra-High Performance Fibre-Reinforced Concrete (UHPFRC 2013)*, F. Toutlemonde and J. Resplendino, eds., Marseille, France pp. 275-284.

Presuel-Moreno, F. J.; Bencosme, R.; Hoque, K.; Nazim, M.; Kazemi, A.; and Tang, F., 2018, "Corrosion Propagation of Carbon Steel Rebars in High Performance Concrete," *BDV27–977–08 Final Report*, Florida Department of Transportation, Tallahassee, FL.

Rizkalla, S.; Zia, P.; Seliem, H.; and Lucier, G., 2005, "Evaluation of MMFX Steel for NCDOT Concrete Bridges," Report No. FHWA/NC/2006-31, North Carolina Department of Transportation, Raleigh, NC, 128 pp.

Shareef, A. Y., 2013, "A Study On Durability Properties of Ultra-High Performance Concrete (UHPC) Utilizing Local Fine Quartz Sand," master's thesis, King Fahd University of Petroleum & Minerals, Dhahran, Saudi Arabia.

Sharma, S.; Arora, V. V.; Kumar, S.; Daniel, Y. N.; and Sharma, A., 2018, "Durability Study of High-Strength Steel Fiber-Reinforced Concrete," *ACI Materials Journal*, V. 115, No. 2, Mar., pp. 219-225. doi: 10.14359/51701122

Soleymani, H. R., and Ismail, M. E., 2004, "Comparing Corrosion Measurement Methods to Assess the Corrosion Activity of Laboratory NC and HPC Concrete Specimens," *Cement and Concrete Research*, V. 34, No. 11, pp. 2037-2044. doi: 10.1016/j.cemconres.2004.03.008

Sritharan, S., 2015, "Design of UHPC Structural Members: Lessons Learned and ASTM Test Requirements," *Advances in Civil Engineering Materials*, V. 4, No. 2, pp. 113-131. doi: 10.1520/ACEM20140042

Tan, Q., 2015, "Investigation of Durability and Compressive Strength of HPC Mixtures and Modeling the Corrosion Initiation Time Through the Electrical Resistivity," master's thesis, California State University, Fullerton, Fullerton, CA.

Wang, B., 2019, "Corrosion Behavior of Corrosion-Resistant Steel Reinforcements in High and Ultra-High-Performance Concrete in Chloride Attack Environments," PhD dissertation, University of Houston, Houston, TX.

Wang, B.; Belarbi, A.; Dawood, M.; and Kahraman, R., 2022, "Corrosion Behavior of Corrosion-Resistant Steel Reinforcements in Normal-Strength and High-Performance Concrete: Large-Scale Column Tests and Analysis," *ACI Materials Journal*, V. 119, No. 5, Sept., pp. 89-102.

Zou, Y.; Wang, J.; and Zheng, Y. Y., 2011, "Electrochemical Techniques for Determining Corrosion Rate of Rusted Steel in Seawater," *Corrosion Science*, V. 53, No. 1, pp. 208-216. doi: 10.1016/j.corsci.2010.09.011